A 3D printed custom-made mask model for frameless neuronavigation during retrosigmoid craniotomy.
A preclinical cadaveric feasibility study

Ann Ital Chir, 2020 91, 5: 526-533
pii: S0003469X20032844
free reading: www.annitalchir.com

Pietro Canzi*, Irene Avato*/**, Stefania Marconi***, Mattia Del Maestro*/°, Alice Giotta Lucifero°°, Marianna Magnetto*, Elena Carlotto*, Ferdinando Auricchio***, Sabino Luzzi°/°°, Marco Benazzo*

**Department of Otorhinolaryngology, University of Pavia, Foundation IRCCS Policlinico "San Matteo", Pavia, Italy*
***School in Experimental Medicine, Department of Clinical-Surgical, Diagnostic and Pediatric Sciences, University of Pavia, Pavia, Italy*
****Department of Civil Engineering and Architecture, University of Pavia, Pavia, Italy*
°Neurosurgery Unit, Department of Surgical Sciences, Fondazione IRCCS Policlinico San Matteo, Pavia, Italy
°°Neurosurgery Unit, Department of Clinical-Surgical, Diagnostic and Pediatric Sciences, University of Pavia, Pavia, Italy

A 3D printed custom-made mask model for frameless neuronavigation during retrosigmoid craniotomy. A preclinical cadaveric feasibility study

BACKGROUND: *A 3D printing custom-made mask model was tested in terms of feasibility and accuracy for frameless neuronavigation during retrosigmoid approach.*
METHODS: *A virtual 3D model of a cadaveric injected head was obtained from a high-resolution Computed Tomography (CT) scan and 3D Printed (3DP). The course of the transverse and sigmoid sinus was marked. A transparent custom-made 3DP mask model was created as a cast of 3D model. The area of the lateral sinuses was grooved to allow the surgeon to use the mask as a template to draw the course of the sinuses on the patient skull. A right retrosigmoid approach was performed on formalin-fixed injected cadaveric head. Inion and other conventional landmarks were used to mark the course of the sinuses. 3DP mask was used to re-mark the course of the sinuses. The mismatch between the landmarks-based and 3DP mask-based track was assumed as a measure of the accuracy of the 3DP mask model.*
RESULTS: *3DP mask model resulted precise, feasible, easy and fast to use. A perfect interlocking with the retrosigmoid area was noted. Mismatch between the landmarks-based and 3DP mask-based track was of 4 and 6 mm for transverse and sigmoid sinus, respectively.*
CONCLUSION: *3DP custom-made mask model is feasible, easily reproducible and reliable for the implementation of a frameless neuronavigation during retrosigmoid approach. Its accuracy is greater than that of the bone landmark neuronavigation. In selected cases, 3DP mask can be a valid option to image-guided optical or electromagnetic tracking systems.*

KEY WORDS: 3D Printing, Neuronavigation, Retrosigmoid Approach, Sigmoid Sinus, Transverse Sinus.

Introduction

The applications of three-dimensional printing (3DP) technology in medical field are numerous, and the usefulness of this know-how has been widely recognized for educational and surgical aims [1-7].

Pervenuto in Redazione Marzo 2020. Accettato per la pubblicazione Aprile 2020
Correspondence to: Alice Giotta Lucifero, Via Fiume 5, 70121 Bari, Italy (e-mail: alicelucifero@gmail.com)

Concerning the educational purposes, the implementation of 3DP models has proved to facilitate the understanding of the three-dimensional anatomy of highly complex districts, especially the skull base [2,3,5]. A second significant area of application is the surgical planning and simulation [6,8]. Concerning the skull base corridors, the retrosigmoid approach encompasses a careful preoperative planning and a precise execution in the light of the risk of injury of the major posterior fossa dural sinuses. The main goal of the retrosigmoid craniotomy is to provide a surgical route which should be as much as possible close to the transverse and sigmoid sinus, practically limiting the need for brain retraction [9]. Bone landmarks-based navigation and image-guided optical and electromagnetic tracking systems are both widely employed in several skull base approaches, being moreover the retrosigmoid approach among those access corridors for which neuronavigation adds substantial advantages. In particular, neuronavigation has been reported to significantly aid the intraoperative localization of the junction between the transverse and sigmoid sinus .[10-16] Nevertheless, the precision of the bony landmarks and the availability of the aforementioned tracking systems has been reported to be limited and, also, not free from errors in cranial and even spinal procedures [17-27]. The accuracy of the optical and electromagnetic systems can be dramatically reduced by mistakes during initial landmarks registration, accidental displacement of the patient head, stretching of the surgical drapes, or also positioning of skin retractors distorting the soft tissues [28].

In this pre-clinical cadaveric study, a 3D printed custom-made mask model for frameless neuronavigation during retrosigmoid approach is tested in terms of feasibility, but also accuracy.

The technical specifics, advantages and limitations of this model are discussed in detail.

Methods

Construction of the Patient 3dp Model

An injected cadaveric head underwent to a high-resolution computed tomography scan (Aquilion One, Toshiba, Tokyo, Japan) (slice thickness 0.5 mm). CT scan images were processed by means of a semi-automatic segmentation method with a free available software (http://www.itksnap.org/pmwiki/pmwiki.php) in order to obtain a virtual 3D model of the skull and neurovascular structures. The virtual model underwent to a further post-processing consisting in contouring the sigmoid and transverse sinus, and tracing both of them on the outer surface of the temporal bone. The model was then printed with a professional 3D printer (ProJet® 460Plus, 3D Systems, Rock Hill, South Carolina, USA), using a binder jetting technology (Fig. 1). This printer had a layer thickness of 100 μm, and employed a chalk-like powder cured with a water-based adhesive, along with ink-jet colors.

Construction Of The 3dp Custom-Made Mask Model

Basing on the 3DP model, a solid mask was then obtained. The outer bony profile of the 3DP model was outlined and extruded of 1 mm, thus obtaining a custom-made mask. The course of the sigmoid and transverse sinus was traced also on the mask. The area corresponding to the sinuses course was removed to create a groove which surgeon can use as a template to draw the course of the sinuses directly on the patient skull. Form2 3D printer (Formlabs, Somerville, Massachusetts, USA) was used to print the mask model by means of a Vat photopolymerization technology, setting a layer thickness of 50 μm. The custom-made mask model was realized with a transparent commercial photopolymer (Accura ClearVue, Formlabs, Somerville, Massachusetts, USA) to preserve the visibility of the underlying anatomical structures (Fig. 2).

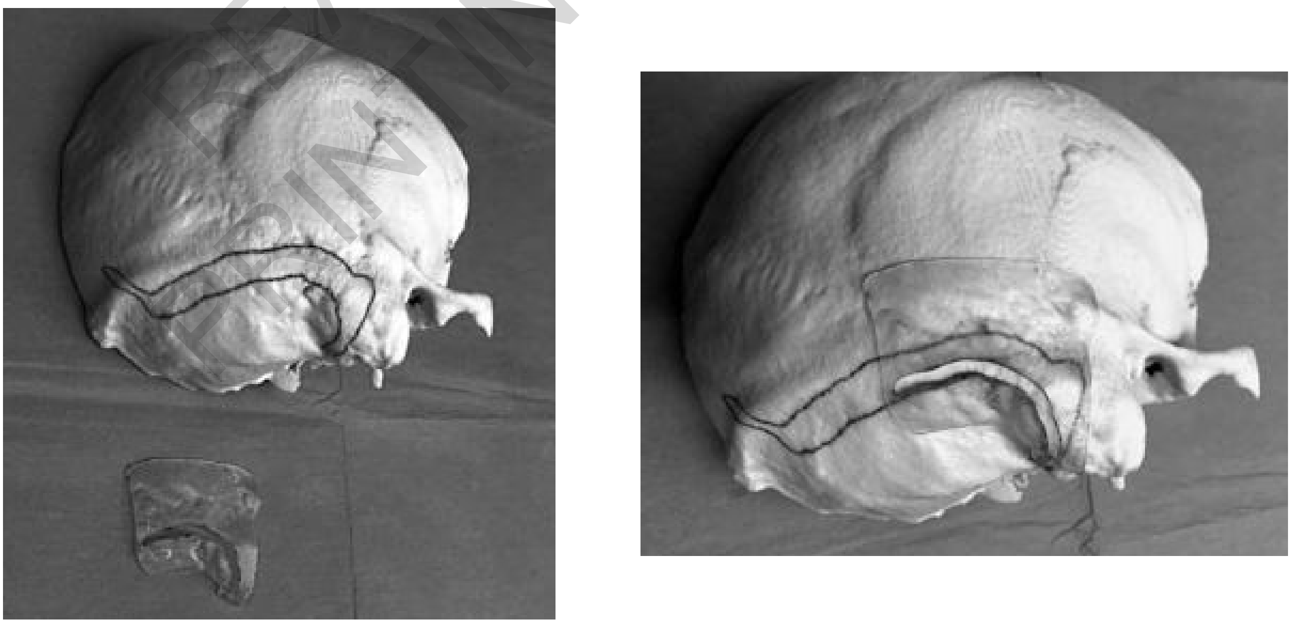

Fig. 1-2: 3DP cadaveric head model and custom-made mask.

Implementation of the 3DP Mask in the Surgical Scenario and Accuracy Check

A formalin-fixed injected head was used for this step. A retrosigmoid approach was performed on the right side. Anatomical landmarks relevant for the retrosigmoid approach were identified on the skin. They were the inion, mastoid tip and posterior root of the zygomatic arc. A line connecting the inion and the posterior root of the zygoma was drawn (Frankfurt plane). In between the middle and lateral two thirds of this line, the asterion was signed. The projection of the sigmoid and transverse sinus was marked on the skin cranial surface using these landmarks (Fig. 3). An italic "S" skin incision was performed, along with a subperiosteal skeletonization of the posterolateral skull base. Lambdoid, occipito-mastoid, parieto-mastoid sutures, and the meeting-point between all of them, namely the asterion, were identified on the bony surface (Fig. 4). Here, the transverse and sigmoid sinus were marked again on the basis of the bony landmarks. Asterion was assumed as the classic landmark for the identification of the junction point between the transverse and sigmoid sinus. The course of the sinuses was marked with a dermographic pencil. 3DP mask model was then fit on the bone in a way such as to allow zero degrees of freedom in a counterclockwise rotation (Fig. 5). The course of the transverse and sigmoid sinuses was re-marked through the groove of the mask (Fig. 6). The mismatch between the landmarks-based line and the 3DP mask-based line was assumed as a measure of the accuracy of the 3DP mask model. Taking into account their different course, the distance between the two lines was measured vertically and horizontally at the midportion of the transverse and sigmoid sinus, respectively. These measures were referred as transverse sinus mismatch distance (TSMD) and sigmoid sinus mis-

Fig. 3: Superficial landmarks for retrosigmoid approach. Projection of the sigmoid and transverse sinus marked on the skin.

Fig. 5: 3DP mask model placed fit on the retrosigmoid area.

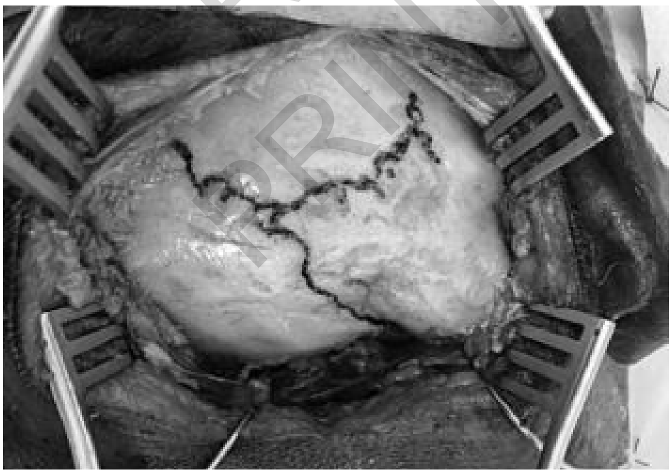

Fig. 4: Retrosigmoid area after the skeletonization. Lambdoid, occipito-mastoid, parieto-mastoid sutures and asterion are marked.

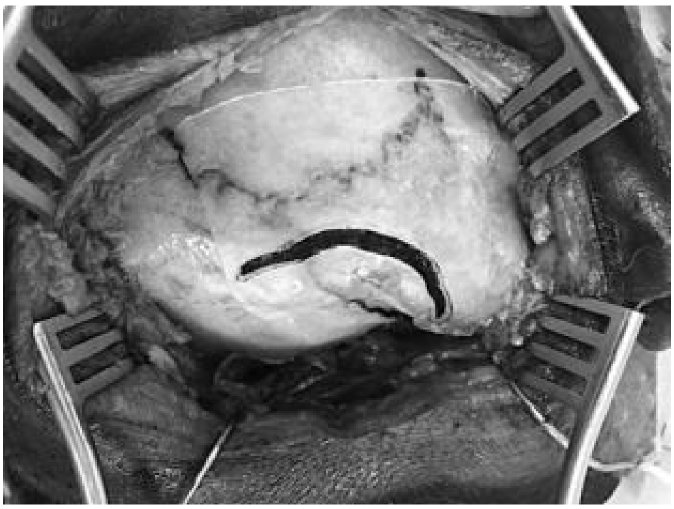

Fig. 6: Transverse and sigmoid sinuses marked through the groove of the mask.

Fig. 7: Mismatch in the identification of the lateral sinuses between bone landmark and 3DP mask navigation. TSMD: transverse sinus mismatch distance; SSMD: sigmoid sinus mismatch distance.

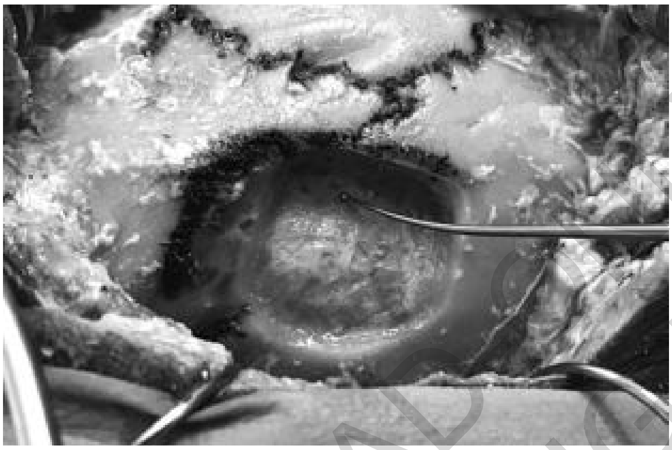

Fig. 8: Exposure of the junction between the transverse and sigmoid sinus after retrosigmoid craniotomy.

match distance (SSMD) (Fig. 7). The retrosigmoid craniotomy was performed on the basis of the line traced by means of the 3DP mask model. Craniotomy involved a single burr hole performed just inferior and medial to the junction point between the sinuses. The successful exposure of the junction between the transverse and sigmoid sinus by means of the burr hole was assumed as a measure of accuracy (Fig. 8).

Results

Feasibility of 3DP Custom-Made Mask Model

The 3DP mask model proved to be feasible, easy and fast to use. After its placement on the bony surface, no counterclockwise rotation was possible because of the overhang of the mastoid and the perfect interlocking of the mask with the retrosigmoid area.

Accuracy of 3DP Custom-Made Mask Model

The single burr hole provided for a full exposure of the junction between the transverse and sigmoid sinus. TSMD and SSMD was 4 and 6 mm, respectively.

Discussion

The retrosigmoid approach is routinely performed by neurosurgeons and neuro-otologists for the treatment of several lesions involving the posterolateral skull base, as it provides a wide exposure of the cerebello-pontine angle [9,29]. Initial steps of the retrosigmoid craniotomy can be challenging and risky for inexperienced surgeons. Retrosigmoid craniotomy has to provide an adequate line of sight to the surgical target, at the same time minimizing the cerebellar retraction. To do this, the first burr hole ought to be located near to the junction between the transverse and sigmoid sinus. The precise intraoperative identification of the venous sinuses is crucial also to prevent catastrophic sequalae coming from their tears [30]. Asterion is classically considered as the most reliable bone landmark to localize the junction between the transverse and sigmoid sinus, although recent studies have questioned its accuracy because of a well-known anatomical individual variability [10,31,32]. Inion, superior nuchal line and zygomatic root are further bone landmarks along the Frankfurt horizontal plane, whilst mastoid tip and digastric groove are considered as additional landmarks specifically for the sigmoid sinus. Dogan et al., suggested to use a line connecting the angle of the mandible and the mastoid tip to localize the external projection of the sigmoid sinus [33]. Zhentao proposed to locate the junction just above a line between the external occipital protuberance and the lowest point of the mastoid process in the coronal and the sagittal planes on 3D CT scan [34]. Although several studies tried to identify new bone landmarks for retrosigmoid approach, or also to validate the existing ones, all of these unfortunately suffer from a not negligible lack of accuracy [17-26]. Moreover, a significant individual, sex- and racial-related variability has been reported [35]. That's the main reason why, by the reason of its high precision and relatively easy of use, image-guided neuronavigation is nowadays routinely employed during surgery of tumors affecting the central nervous system [36-49] , skull base and posterior fossa [50-56], but also aneurysms, arteriovenous and cavernous malformations [57-64].
In addition, the implementation of minimally invasive techniques in several surgical areas [65-70], such as endoscopic and stereotatic procedures, made the employment of neuronavigation even more necessary [12,50,71-77]. The "patient-specificity" of neuronavigation, allows to overcome the aforementioned rate of anatomical variability related to the use of the only bone landmarks.
Furthermore, few doubts do exist about the usefulness

of the navigation in reducing morbidity coming from potential injuries to vital structures.

Despite all these advantages, conventional image-guided neuronavigation systems suffer from some technical weakness. They involve the placement of a skull clamp which, apart from having risks of complications [78], may also potentially interfere with the surgical maneuvers during specific approaches, thus limiting the surgeon and the patient comfort. An additional problem is their accuracy. In 2013, Stieglitz and colleagues published a retrospective quality-control study aimed to quantify the decrease of accuracy of neuronavigation during cranial neurosurgery. They highlighted some pitfalls related to the loss of precision, mainly coming from the patient position, modality of initial registration, surgical draping, placement of skin retractors, along with accidental movements of the patient head, skull clamp and reference arc [28]. In recent years, 3DP technology has lived a tremendous and never seen before development in many medical fields, 3DP models being been trusted as a valuable tool for engineering of bio-scaffolds, preclinical anatomical education, surgical training, preoperative planning and also surgical simulation, suitable for many surgical fields [1,79-89]. Particularly precious has been the employment of the 3DP technology in surgery, because of its high reliability regarding both the morphology and the mechanical properties resembling those of the living tissues. In neurosurgical practice, custom-made models are commonly employed for the construction of biosynthetic and biocompatible cranial flaps after decompressive craniectomy [90]. Furthermore, 3DP models can be used to design preoperatively some custom-made graft to be employed in those challenging cases where a large bony demolition is planned. Just to cite few, they have been recently used to plan the positioning of semi-implantable transcutaneous bone-conduction implants, en bloc resections of primary spine tumors, petroclival lesions, cranioplasty, or also to preoperatively quantify the differences in facial symmetry before reconstructive surgery [2,7,72,91,92]. Last but far from least, 3DP technology has the great advantage to be based on the patient own radiological images, being able to be considered therefore as an image-guided navigation.

The present pre-clinical study allowed to practically assess the feasibility of the 3DP custom-made mask model in the execution of the retrosigmoid approach. The measured TSMD and SSMD allowed to consider the present model more accurate in comparison with the bone landmarks-based navigation. Noteworthy, the implementation of the mask was fast and user friendly. In the light of these evidences, 3DP mask model may be considered a valuable option to conventional image-guided neuronavigation systems in selected cases.

However, some limitations of this model have to be mentioned. First, it can be used only in elective cases; second, the projection of the sigmoid and transverse sinus must be done taking into account the surgical position, otherwise, the spatial information would be improper. In addition, observation on a larger scale are necessary to definitively confirm our data regarding the accuracy.

Conclusions

The reported 3DP custom-made mask model has proved to be easily reproducible and reliable for the implementation of a frameless neuronavigation during retrosigmoid approach.

The mask allows to estimate the projection of the transverse and sigmoid sinuses on the bony surface with an accuracy greater than that provided by the use of the only bone landmarks.

The use of this mask model allows to reduces the potential risks related to an accidental slippage of the headframe and, ultimately, permits to perform a precise and safe retrosigmoid craniotomy.

3DP custom-made mask model should be considered as an additional tool for neuro-otologists and neurosurgeons, to be used in selected cases as a valid option to image-guided optical or electromagnetic tracking systems.

Riassunto

Un modello di maschera personalizzato realizzato mediante l’utilizzo di stampante 3D è stato testato in termini di fattibilità e precisione ai fini della neuronavigazione frameless durante l'esecuzione dell’approccio retrosigmoideo.

Un modello virtuale è stato ottenuto e stampato in 3D a partire da una testa di cadavere iniettata, fissata in formalina, e sottoposta a tomografia computerizzata ad alta risoluzione. Il decorso del seno trasverso e sigmoideo è stato disegnato sulla sagoma 3D. Sulla scorta del modello una maschera 3D custom-made trasparente è stata successivamente prodotta con una scanalatura in corrispondenza dell’area dei seni laterali per consentire al chirurgo di tracciare durante l’approccio il decorso dei seni direttamente sul cranio del paziente. È stato dunque eseguito un accesso retrosigmoideo destro sulla testa del cadavere. L’inion e gli altri principali reperi ossei convenzionali sono stati usati per delineare il decorso dei seni venosi durali. Successivamente la maschera 3D è stata impiegata per ridisegnare il decorso dei seni. La discrepanza tra le due tracce è stata assunta come misura dell'accuratezza del modello.

Il modello di maschera 3D è risultato preciso, affidabile, facile e veloce da utilizzare. È stata inoltre documentata una perfetta corrispondenza con l'area retrosigmoidea. La differenza tra le due tracce è stata di 4 mm per il seno trasverso e di 6 mm per quello retrosigmoideo.

Il modello di maschera 3D custom made è risultato fattibile, facilmente riproducibile e affidabile ai fini dell’implementazione della neuronavigazione frameless

durante l'approccio retrosigmoideo. La sua precisione è stata maggiore di quella della neuronavigazione basata su reperi ossei. In casi selezionati la maschera 3D può essere un'opzione valida rispetto ai sistemi di neuronavigazione ottica ed elettromagnetica guidati da immagini.

References

1. Canzi P, et al.: *New frontiers and emerging applications of 3D printing in ENT surgery: A systematic review of the literature.* Acta Otorhinolaryngol Ital, 2018; 38(4): 286-303.

2. Ahmed AK, et al.: *Multidisciplinary surgical planning for en bloc resection of malignant primary cervical spine tumors involving 3D-printed models and neoadjuvant therapies: report of 2 cases.* J Neurosurg Spine, 2019: 1-8.

3. Thawani JP, et al.: *Three-dimensional printed modeling of an arteriovenous malformation including blood flow.* World Neurosurg, 2016. 90:675-683 e2.

4. Thawani JP, et al.: *Three-dimensional printed modeling of diffuse low-grade gliomas and associated white matter tract anatomy.* Neurosurgery, 2017; 80(4): 635-45.

5. Yi X, et al.: *Three-dimensional printed models in anatomy education of the ventricular system: A randomized controlled study.* World Neurosurg, 2019; 125: e891-e901.

6. Mooney MA, et al.: *Three-dimensional printed models for lateral skull base surgical training: Anatomy and simulation of the transtemporal approaches.* Oper Neurosurg (Hagerstown), 2020; 18(2): 193-201.

7. Muelleman TJ, et al.: *Individualized surgical approach planning for petroclival tumors using a 3d printer.* J Neurol Surg B Skull Base, 2016; 77(3):243-48.

8. Hsieh TY, et al.: *Assessment of a patient-specific, 3-dimensionally printed endoscopic sinus and skull base surgical model.* JAMA Otolaryngol Head Neck Surg, 2018; 144(7):574-79.

9. Elhammady MS, Telischi FF, Morcos JJ: *Retrosigmoid approach: Indications, techniques, and results.* Otolaryngol Clin North Am, 2012; 45(2): 375-97, ix.

10. Day JD, Tschabitscher M: *Anatomic position of the asterion.* Neurosurgery, 1998; 42(1): 198-99.

11. Sheng B, et al.: *Anatomical relationship between cranial surface landmarks and venous sinus in posterior cranial fossa using CT angiography.* Surg Radiol Anat, 2012; 34(8): 701-8.

12. da Silva EB Jr, et al.: *Image-guided surgical planning using anatomical landmarks in the retrosigmoid approach.* Acta Neurochir (Wien), 2010; 152(5): 905-10.

13. Matsushima K, et al.: *Microsurgical and Endoscopic Anatomy for Intradural Temporal Bone Drilling and Applications of the Electromagnetic Navigation System: Various Extensions of the Retrosigmoid Approach.* World Neurosurg, 2017; 103:620-30.

14. Sjolund LA, Kell PDy, McNamara TP: *Optimal combination of environmental cues and path integration during navigation.* Mem Cognit, 2018; 46(1): 89-99.

15. Kelly PD, K.J, S. Doucet St, Luke A: *Exploring the roles, functions, and background of patient navigators and case managers: A scoping review.* Int J Nurs Stud, 2019; 98:27-47.

16. Kelly PD, et al.: *Image guidance in spine tumor surgery.* Neurosurg Rev, 2019.

17. Avci E, et al.: *Lateral posterior fossa venous sinus relationships to surface landmarks.* Surgical neurology, 2003; 59(5): 392-97.

18. Duangthongpon P, et al.: *The Relationships between Asterion, the Transverse-Sigmoid Junction, the Superior Nuchal Line and the Transverse Sinus in Thai Cadavers: Surgical Relevance.* Journal of the Medical Association of Thailand = Chotmaihet thangphaet, 2016; (99) Suppl 5: S127-S131.

19. Tubbs RS, et al.: *Surface landmarks for the junction between the transverse and sigmoid sinuses: Application of the "strategic" burr hole for suboccipital craniotomy.* Neurosurgery, 2009; 65(6 Suppl): 37-41.

20. Galindo-de León S, et al.: *Morphometric characteristics of the anterior and the posterolateral surface of the skull: its relationship with dural venous sinuses and its neurosurgical importance.* Cirugia y cirujanos, 2013; 81(4): 69-73.

21. Hall S, Peter Gan YC, *Anatomical localization of the transverse-sigmoid sinus junction: Comparison of existing techniques.* Surgical neurology international, 2019; 10: 186-86.

22. Hwang RS, et al.: *Relationship of the sinus anatomy to surface landmarks is a function of the sinus size difference between the right and left side: Anatomical study based on CT angiography.* Surgical neurology international, 2017; 8: 58-58.

23. Li RC, et al.: *Localization of anterosuperior point of transverse-sigmoid sinus junction using a reference coordinate system on lateral skull surface.* Chinese medical journal, 2016; 129(15): 1845-849.

24. Xia L, et al.: *Localization of transverse-sigmoid sinus junction using preoperative 3D computed tomography: application in retrosigmoid craniotomy.* Neurosurgical review, 2012; 4): 593-99.

25. Mascott CR, et al.:*Quantification of true in vivo (application) accuracy in cranial image-guided surgery: influence of mode of patient registration.* Neurosurgery, 2006; 59(1 Suppl 1): ONS146-ONS156.

26. Grauvogel TD, et al.: *Navigation accuracy after automatic- and hybrid-surface registration in sinus and skull base surgery.* PloS one, 2017; 12(7): e0180975-e0180975.

27. Millimaggi DF, et al.: *Minimally invasive transforaminal lumbar interbody fusion with percutaneous bilateral pedicle screw fixation for lumbosacral spine degenerative diseases. A retrospective database of 40 consecutive cases and literature review.* Turk Neurosurg, 2018; 28(3): 454-61.

28. Stieglitz LH, et al.: *The silent loss of neuronavigation accuracy: A systematic retrospective analysis of factors influencing the mismatch of frameless stereotactic systems in cranial neurosurgery.* Neurosurgery, 2013; 72(5): 796-807.

29. Wang C, et al.: *Clinical application of scalp markers and three-dimensional sliced computed tomography reconstructions of the skull transverse-sigmoid sinus groove in the retrosigmoid approach.* Turk Neurosurg, 2018; 28(3): 356-63.

30. Xia L, et al.: *Localization of transverse-sigmoid sinus junction using preoperative 3D computed tomography: Application in retrosigmoid craniotomy.* Neurosurg Rev, 2012; 35(4): 593-98; discussion 598-99.

31. Day J.D.a.K.J.X.a.T.M.a.F.T: *Surface and superficial surgical anatomy of the posterolateral cranial base: significance for surgical planning and approach.* Neurosurgery, 1996; 38(6): 1079-83; discussion 1083-4.

32. Ucerler H, Govsa F: *Asterion as a surgical landmark for lateral cranial base approaches.* J Craniomaxillofac Surg, 2006; 34(7): 415-20.

33. Dogan I, et al.: *Preoperative exposure of sigmoid sinus trajectory in posterolateral cranial base approaches using a new landmark through a neurosurgical perspective.* J Craniofac Surg, 2018; 29(1): 220-25.

34. Yu Z, et al.: *Morphologic study of positional relationship between transverse-sigmoid sinus and extracranial bony landmarks with reconstructed computed tomographic image.* J Craniofac Surg, 2016; 27(7): 1849-853.

35. Dao Trong, P, et al.: *Racial differences in the anatomy of the posterior fossa: Neurosurgical considerations.* World Neurosurg, 2018; 117: e571-e574.

36. Zoia C, et al.: *Sacral solitary fibrous tumour: surgery and hadrontherapy, a combined treatment strategy.* Reports of Practical Oncology & Radiotherapy, 2020.

37. Campanella R, et al.: *Tumor-educated platelets and angiogenesis in glioblastoma: another brick in the wall for novel prognostic and targetable biomarkers, changing the vision from a localized tumor to a systemic pathology.* Cells, 2020; 9(2).

38. Antonosante, A, et al.: *Autocrine CXCL8-dependent invasiveness triggers modulation of actin cytoskeletal network and cell dynamics.* Aging (Albany NY), 2020; 12.

39. Spena, G, et al.: *Risk factors for intraoperative stimulation-related seizures during awake surgery: An analysis of 109 consecutive patients.* J Neurooncol, 2019.

40. Palumbo P, et al.: *NOS2 inhibitor 1400W induces autophagic flux and influences extracellular vesicle profile in human glioblastoma u87mg cell line.* Int J Mol Sci, 2019; 20(12).

41. Luzzi, S, et al.: *Anterolateral approach for retrostyloid superior parapharyngeal space schwannomas involving the jugular foramen area: A 20-year experience.* World Neurosurg, 2019.

42. Luzzi S, et al.: *Dysembryoplastic neuroepithelial tumors: what you need to know.* World Neurosurg, 2019; 127: 255-65.

43. Luzzi S, et al.: *The cell-based approach in neurosurgery: ongoing trends and future perspectives.* Heliyon, 2019; 5(11).

44. Bellantoni G, et al: *Simple schwannomatosis or an incomplete Coffin-Siris? Report of a particular case.* eNeurologicalSci, 2019; 14: 31-33.

45. Zoia C, et al.: *Outcome of elderly patients undergoing intracranial meningioma resection: A single center experience.* J Neurosurg Sci, 2018.

46. Palumbo P, et al.: *Invo:lvement of NOS2 activity on human glioma cell growth, clonogenic potential, and neurosphere generation.* Int J Mol Sci, 2018; 19(9).

47. Luzzi, S, et al:*Engraftment, neuroglial transdifferentiation and behavioral recovery after complete spinal cord transection in rats.* Surg Neurol Int, 2018; 9: 19.

48. Cheng CY, R Shetty, Sekhar LN: *Microsurgical resection of a large intraventricular trigonal tumor: 3-dimensional operative video.* Oper Neurosurg (Hagerstown), 2018; 15(6):E92-E93.

49. Raysi Dehcordi S, et al.: *Stemness marker detection in the periphery of glioblastoma and ability of glioblastoma to generate glioma stem cells: clinical correlations.* World Neurosurg, 2017; 105: 895-905.

50. Chartrain AG, et al.: *A review and comparison of three neuronavigation systems for minimally invasive intracerebral hemorrhage evacuation.* J Neurointerv Surg, 2018; 10(1): 66-74.

51. Pillai P, Sammet S, Ammirati M: *Application accuracy of computed tomography-based, image-guided navigation of temporal bone.* Neurosurgery, 2008; 63(4 Suppl 2): 326-33.

52. Komune N, et al.: *The accuracy of an electromagnetic navigation system in lateral skull base approaches.* The Laryngoscope, 2017; 127(2): 450-59.

53. Pillai P, Sammet S, Ammirati M: *Image-guided, endoscopic-assisted drilling and exposure of the whole length of the internal auditory canal and its fundus with preservation of the integrity of the labyrinth using a retrosigmoid approach: A laboratory investigation.* Neurosurgery, 2009; 65(6 Suppl): 53-59.

54. Selesnick SH, Kacker A: *Image-guided surgical navigation in otology and neurotology.* The American journal of otology, 1999; 20(5): 688-697.

55. Dolati P, et al.: *Multimodal navigated skull base tumor resection using image-based vascular and cranial nerve segmentation: A prospective pilot study.* Surgical neurology international, 2015; 6: 172-72.

56. Colasanti R, et al.: *Image-guided, microsurgical topographic anatomy of the endolymphatic sac and vestibular aqueduct via a suboccipital retrosigmoid approach.* Neurosurgical review, 2015; 38(4):715-21.

57. Luzzi S, et al.: *Letter to the editor regarding "One and done: Multimodal treatment of pediatric cerebral arteriovenous malformations in a single anesthesia event".* World Neurosurg, 2020; 134: 660.

58. Luzzi, S, et al.: *Indication, timing, and surgical treatment of spontaneous intracerebral hemorrhage: Systematic review and proposal of a management algorithm.* World Neurosurg, 2019.

59. Luzzi S, Del Maestro M, Galzio R: *Letter to the Editor. Preoperative embolization of brain arteriovenous malformations.* J Neurosurg, 2019: 1-2.

60. Luzzi S, et al.: *Giant and very large intracranial aneurysms: surgical strategies and special issues.* Acta Neurochir Suppl, 2018; 129: 25-31.

61. Luzzi S, et al.: *Onyx embolization before the surgical treatment of grade III spetzler-martin brain arteriovenous malformations: single-center experience and technical nuances.* World Neurosurg, 2018; 116: e340-e353.

62. Gallieni M, et al.: *Endoscope-Assisted microneurosurgery for intracranial aneurysms: Operative technique, reliability, and feasibility based on 14 years of personal experience.* Acta Neurochir Suppl, 2018; 129:19-24.

63. Del Maestro M, et al.: *Surgical treatment of arteriovenous malformations: role of preoperative staged embolization.* Acta Neurochir Suppl, 2018; 129: 109-13.

64. Ricci A, et al.: *Cortical aneurysms of the middle cerebral artery: A review of the literature.* Surg Neurol Int, 2017; 8: 117.

65. Tartaglia N, et al.: *Robotic voluminous paraesophageal hernia repair: A case report and review of the literature.* J Med Case Rep, 2020; 14(1): 25.

66. Di Lascia A, et al.: *Endoscopy for treating minor post-cholecystectomy biliary fistula A review of the literature.* Ann Ital Chir, 2018; 89: 270-77.

67. Cianci P, et al.: *T-tube biliary drainage during reconstruction after pancreaticoduodenectomy. A single-center experience.* Ann Ital Chir, 2017; 88: 330-35.

68. Tartaglia N, et al.: *Laparoscopic antegrade cholecystectomy: A standard procedure?* Open Med (Wars), 2016; 11(1): 429-32.

69. Neri V, et al.: *Laparoscopic cholecystectomy: evaluation of liver function tests.* Ann Ital Chir, 2014; 85(5): 431-37.

70. Tartaglia N, et al.: *Acute suppurative thyroiditis after fine needle aspiration. Case report and literature review.* Chirurgia, 2017; June: 89-94.

71. Minkin K, et al.: *Three-dimensional neuronavigation in SEEG-guided epilepsy surgery.* Acta Neurochir (Wien), 2019; 161(5): 917-23.

72. Park SE, et al.: *Modified cranioplasty technique using 3-dimensional printed implants in preventing temporalis muscle hollowing.* World Neurosurg, 2019; 126: e1160-e1168.

73. Arnaout MM, et al.: *Supraorbital keyhole approach: Pure endoscopic and endoscope-assisted perspective.* Clin Neurol Neurosurg, 2019; 189: 105623.

74. Luzzi S, et al.: *Morphometric and radiomorphometric study of the correlation between the foramen magnum region and the anterior and posterolateral approaches to ventral intradural lesions.* Turk Neurosurg, 2019.

75. Luzzi S, et al.: *Endoscope-assisted microneurosurgery for neurovascular compression syndromes: basic principles, methodology, and technical notes.* Asian J Neurosurg, 2019; 14(1): 193-200.

76. Luzzi, S, et al.: *Lateral transorbital neuroendoscopic approach for intraconal meningioma of the orbital apex: Technical nuances and literature review.* World Neurosurg, 2019; 131: 10-17.

77. Zoia C, et al.: *Transnasal endoscopic removal of a retrochiasmatic cavernoma: A case report and review of literature.* Surg Neurol Int, 2019; 10: 76.

78. Bongetta D, et al.: *Neurosurgical issues of bariatric surgery: A systematic review of the literature and principles of diagnosis and treatment.* Clin Neurol Neurosurg, 2019; 176: 34-40.

79. Liaw CY, Guvendiren M: *Current and emerging applications of 3D printing in medicine.* Biofabrication, 2017; 9(2): 024102-024102.

80. Scoutaris N, Ross S, Douroumis D: *Current trends on medical and pharmaceutical applications of inkjet printing technology.* Pharmaceutical research, 2016; 33(8): 1799-816.

81. Trenfield SJ, et al.: *Shaping the future: Recent advances of 3D printing in drug delivery and healthcare.* Expert opinion on drug delivery, 2019; 16(10): 1081-1094.

82. Nagarajan N, et al.: *Enabling personalized implant and controllable biosystem development through 3D printing.* Biotechnology advances, 2018; 36(2): 521-33.

83. Alhnan MA, et al.: *Emergence of 3D printed dosage forms: opportunities and challenges.* Pharmaceutical research, 2016; 33(8): 1817-832.

84. Ji S, Guvendiren M: *3D printed wavy scaffolds enhance mesenchymal stem cell osteogenesis.* Micromachines, 2019; 11(1): 31.

85. Tartaglia N, et al.: *Bilateral central neck dissection in the treatment of early unifocal papillary thyroid carcinomas with poor risk factors A mono-institutional experience.* Ann Ital Chir, 2019; 8.

86. Cianci P, et al.: *Cervical esophagotomy for foreign body extraction: a case report and extensive literature review of the last 20 years.* Am J Case Rep, 2018; 19: 400-405.

87. Tartaglia N, et al: *What is the treatment of tracheal lesions associated with traditional thyroidectomy? Case report and systematic review.* World J Emerg Surg, 2018; 13: 15.

88. Sanguedolce, F, et al.: *Bladder metastases from breast cancer: managing the unexpected. A systematic review.* Urol Int, 2018; 101(2): 125-31.

89. Tartaglia N, et al.: *One stage surgery for synchronous liver metastasis from a neuroendocrine tumor of the colon. A case report.* Ann Ital Chir, 2017; 6.

90. Elsawa Y, et al.: *Early decompressive craniectomy as management for severe tbi in the pediatric population: A comprehensive literature review.* World Neurosurg, 2020.

91. Canzi P, et al.: *From CT scanning to 3D printing technology: A new method for the preoperative planning of a transcutaneous bone-conduction hearing device.* Acta Otorhinolaryngol Ital, 2018; 38(3): 51-56.

92. Arias E, et al.: *Virtual surgical planning and Three-dimensional printed guide for soft tissue correction in facial asymmetry.* J Craniofac Surg, 2019; 30(3): 846-50.